

강한 지진하중하에서 강부재의 정량적인 손상 모델

Quantitative Damage Model of Steel Members under Severe Seismic Loading

박 연 수¹⁾ · 박 선 준²⁾

Park, Yeon Soo Park, Sun Joon

요 약 : 본 논문에서는 정량적인 지진 손상모델의 유도를 위해 먼저 지진 반복하중하에서 구조물 및 그들 요소에 대한 기존의 손상 모델들을 체계적으로 정리한 후 문제점을 평가하였다. 또한, 강한 지진과 같은 심한 반복가력을 받는 강구조 부재에 대한 파괴기준을 묘사하였으며, 강부재에 대한 새로운 지진 손상도 평가방법을 제안하였다. 이 손상모델은 극저 사이클 하중하에서 강부재에 대한 일련의 실험과 수치해석 연구로부터 얻어진 것이다. 본 연구에서 극저 사이클 하중은 큰 소성변형 영역안에서 5~20 사이클의 반복하중을 의미한다. 제안된 내진 손상평가 방법은 변형이 가장 심하게 집중된 단면에 있어서 국소 변형율의 이력에 초점을 맞추어 유도되었다.

ABSTRACT : In this paper, the previous damage models for structures and their components under seismic repeated loading were reviewed systematically. A failure criterion for steel members under severe cyclic excitations as in strong earthquakes was described. A new approach to seismic damage assessment for steel members was proposed. This method was based on a series of the experimental and numerical investigations for steel members under very low cyclic loading. In this study, very low cyclic loading means repetitive loading, 5 to 20 loading cycles, within the large plastic range. The proposed damage assessment method was focused on the local strain history at the cross-section of the most severe concentration of deformation.

핵심용어 : 손상모델, 손상지수, 강구조물, 부재, 지진반복하중, 극저사이클 하중, 국소 변형율, 균열

KEYWORDS : damage model, damage index, steel structure, member, seismic repeated loading, very low cycle loading, local strain, cracking

1) 정회원, 전남대학교 공과대학 토목공학과 교수
2) 정회원, 전남대학교 토목공학과 박사과정

본 논문에 대한 토의를 1999년 3월 31일까지 학회로 보내주시면 토의 회답을 게재하겠습니다.

1. Introduction

In the last 30 years, numerous approaches to seismic damage assessment have been proposed. This damage evaluation has been accompanied with high-storied and large-scalization in civil engineering structures such as bridges, buildings, offshore oil and gas platforms, nuclear power plants and so on. Although a lot of researches, both experimental and analytical, has been carried out to make an exact model or method to seismic damage assessment for structures and their members, a decisive one is not developed yet.

Therefore it is necessary to develop a new damage assessment method considering exactly the physical aspects of seismic damage and failure mechanisms for structures and their members, which may finally be able to improve general reliability and damage estimation against earthquakes⁽¹⁾.

It is obvious for economically-designed steel structures that brittle failure in welded connections or elastic instability failure is not a serious problem. The most important thing is to clarify the inelastic post-buckling behavior of members under repeated loading. In order to establish a safety assessment criterion for steel structures under severe seismic excitations, the structural behavior at the critical section of members under very low cycles of loading must be considered⁽¹⁾. The reason is because structural damage and failure are often associated with plastic and/or unstable behavior of structural members due to large cyclic deformations

with initiation of local buckling. The structural behavior at the critical section should be related to the local strain or stress at the critical cross-section of structures and their members. Thus, it appeared to the writers that the damage criterion at the point of the local strain history of the critical cross-section is required to estimate the seismic safety more precisely.

A new approach to seismic safety assessment for steel members was proposed herein. This method was based upon a series of the experimental and numerical investigations for steel angle members under very low cycles of loading. Importance of local strain parameter was discussed in relation to cracking to identify a quantitative relationship between damage and itself. The proposed seismic damage model is focused on the local strain history at the cross-section of the most severe concentration of local deformation.

2. Review of Damage Models under Repeated Loading

In order to understand the damage models that have been proposed previously, it is necessary to clarify the damage indices according to the used variables for damage assessment. The damage indices are usually defined as the damage values normalized with respect to the failure level so that a damage index value of unity corresponds to the failure. Tables 1~5 show a systematic classification of

the local and global damage indices for steel structures, reinforced concrete structures, and their components subjected to cyclic loading, which have been proposed during the past 30 years. Here the local and global damage indices are defined as the damage indices for a individual component, i.e. structural element or member, and total structure combined with these components, respectively. All of these are categorized into four groups: (1) damage indices based on the variable of ductility ratio (see Table 1), (2) damage indices

based on the variable of stiffness degradation (see Table 2), (3) damage indices based on the variable of dissipated energy (see Table 3), and damage indices based on the linear combination of ductility ratio and dissipated energy (Table 4).

The damage indices based on ductility ratios are one of the first proposals to assess the damage contents due to cyclic loads (see Table 1). These indices are basically related to a ratio of the capacity (plastic strain) and demand (largest plastic strain resulting from cyclic loads)

Table 1. Local damage indices based on ductility ratio

Proposer	Equation	Remarks
Yao & Munse (1962)	$D = \sum_{i=1}^n \left(\frac{\Delta q_{t,i}}{\Delta q_{n,i}} \right)^{1/m}$	D : cumulative damage ranged from 0.0 - 1.0 n : number of cycles $\Delta q_{t,i}$: incremental positive plastic strain during <i>i</i> -th cycle $\Delta q_{n,i}$: tension plastic strain to cause failure during <i>i</i> -th cycle m : material constant object : for structural steel components
Bertero & Bresler (1977)	$D_i = \frac{d_i}{c_i}$	D_i : damage index for a given element <i>i</i> d_i : response(demand) of the element <i>i</i> c_i : resistance(capacity) of the element <i>i</i> object : for reinforced concrete members
Banon, Biggs & Irvine (1981)	$\mu_\theta = \frac{\theta_{max}}{\theta_y}$ $\mu_\phi = \frac{\phi_{max}}{\phi_y}$ $NCR = \frac{\sum \theta_o }{\theta_y}$	μ_θ : rotation ductility θ_{max} : maximum rotation θ_y : yield rotation μ_ϕ : curvature ductility ϕ_{max} : maximum curvature ϕ_y : yield curvature NCR : normalized cumulative rotation θ_o : plastic rotation object : for reinforced concrete members
Krawinkler & Zohrei (1983)	$D = C \sum_{i=1}^n (\Delta \delta_{pi})^c$	D : cumulative damage index of member C, c : damage parameters $\Delta \delta_{pi}$: plastic strain during the <i>i</i> -th cycle object : for structural steel component
Stephens & Yao (1987)	$D = \sum_{i=1}^n \left(\frac{\Delta \delta_{pi,i}}{\Delta \delta_{fi,i}} \right)^a$ where, $a = 1 - b \times \frac{\Delta \delta_{pc,i}}{\Delta \delta_{pt,i}}$	D : damage for all <i>n</i> cycles $\Delta \delta_{pc,i}$: negative change in plastic deformation in the <i>i</i> -th cycle $\Delta \delta_{pt,i}$: positive change in plastic deformation in the <i>i</i> -th cycle $\Delta \delta_{fi,i}$: positive change in plastic deformation to cause failure in the <i>i</i> -th cycle b : deformation ratio coefficient object : for reinforced concrete members

Table 2. Local damage indices based on stiffness degradation

Proposer	Equation	Remarks
Lybas & Sozen (1979)	$DR = \frac{K_o}{K_r}$	DR : damage ratio K_o : initial tangent stiffness K_r : reduced secant stiffness corresponding to maximum displacement object : for reinforced concrete members
Roufaiel & Myer (1987)	$MFDR = \max[MFDR^+, MFDR^-]$ where, $MFDR^+ = \frac{\frac{\phi_x^+}{M_x^+} - \frac{\phi_y^+}{M_y^+}}{\frac{\phi_m^+}{M_m^+} - \frac{\phi_y^+}{M_y^+}}$ $MFDR^- = \frac{\frac{\phi_x^-}{M_x^-} - \frac{\phi_y^-}{M_y^-}}{\frac{\phi_m^-}{M_m^-} - \frac{\phi_y^-}{M_y^-}}$	M_o/ϕ_o : initial elastic stiffness M_x/ϕ_x : secant stiffness at arbitrary local level M_m/ϕ_m : secant stiffness at onset of failure + and - : loading direction MFDR=1 signifies the onset of failure object : for reinforced concrete members

of structural components. This concept has been modified to contain the effect of cumulative damages by Yao and Munse⁽²⁾, Kasiraj and Yao⁽³⁾, Bertero and Bresler⁽⁴⁾, Blejwas and Bresler⁽⁵⁾ and Stephens and Yao⁽⁶⁾. In these damage models, however, it does not consider the effects of the loading sequence and the local instabilities in the plastic region of members accumulated by repeated loading.

Lybas and Sozen⁽⁷⁾, Meyer and Roufaiel⁽⁸⁾, and Roufaiel and Meyer⁽⁹⁾ developed another types of damage indices connected with stiffness degradations, which presented the damage states as a simple ratio of stiffness (see Table 2). These types of damage indices cannot be used as an exact damage predictor under inelastic cyclic loading because of no consideration of the cumulative state of damage.

Gosain et al.⁽¹⁰⁾ proposed an energy index for seismic damage assessment. In recent years, many proposals for damage

assessment associated with the dissipated energy have been made by Banon et al.⁽¹¹⁾, Hwang and Scribner⁽¹²⁾, Darwin and Nmai⁽¹³⁾, and Chung et al.⁽¹⁴⁾. As pointed out in the above investigations, the energy dissipation capacity has been shown to have a potentially important influence on the damage of reinforced concrete members during strong earthquakes (see Table 3). Namely, these concepts seem to be very attractive for the derivation of a reliable damage model for reinforced concrete members. But it is extremely difficult to present the relationship between the damage level and the dissipated energy, since the number of cycles to failure and total energy dissipation capacity are not corresponding one-to-one.

Park et al.⁽¹⁵⁾, and Nishigaki and Mizuhata⁽¹⁶⁾ introduced a seismic damage model for reinforced concrete members including the ductility ratio and dissipated

Table 3. Local damage indices based on dissipated energy

Proposer	Equation	Remarks
Gosain, Brown & Jiras (1977)	$I_w = \sum_{i=1}^n \frac{P_i \Delta_i}{P_y \Delta_y}$	I_w : work index n : number of load cycles in which $P/P_y > 0.75$ P_i, Δ_i : load and corresponding displacement during i -th cycle P_y, Δ_y : load and corresponding displacement at yield of flexural bars object : for reinforced concrete members
Banon, Biggs & Irvine (1981)	$E_n(t) = \frac{\int_0^t M(\tau)\theta(d\tau)}{\frac{M_y \theta_y}{2}}$	$E_n(t)$: normalized dissipated energy as a function of time "t" t : elapse time M : moment θ : rotation M_y : yield moment θ_y : yield rotation object : for reinforced concrete members
Hwang & Scriber (1984)	$I_E = \sum_{i=1}^n E_i \cdot \frac{K_i}{K_e} \cdot \left(\frac{\Delta_i}{\Delta_y}\right)^2$	I_E : energy index E_i : energy dissipated during the i -th cycle K_e, Δ_e : elastic stiffness and yield deflection, respectively K_i, Δ_i : flexural stiffness and maximum displacement in the i -th cycle, respectively n : number of cycles with $P \geq 0.75P_y$ object : for reinforced concrete members
Darwin & Nmai (1986)	$D_i = \frac{E}{0.5P_y \Delta_y \left[1 + \left(\frac{A_s'}{A_s}\right)^2 \right]}$	D_i : normalized dissipated energy index E : total dissipated energy A_s', A_s : area of compression and tension steel, respectively P_y : yield load Δ_y : yield deflection object : for reinforced concrete members
Chung, Meyer, & Shinozuka (1987)	$D_e = \sum_i \sum_j \left(a_{ij}^+ \frac{n_{ij}^+}{N_i^+} + a_{ij}^- \frac{n_{ij}^-}{N_i^-} \right)$	D_e : cumulative damage index i : indicator of different displacement or curvature level j : indicator of cycle number for given load level i N_i : number of cycles (with curvature level i) to cause failure n_{ij} : number of cycles (with curvature level i) actually applied a_{ij} : damage accelerator $+, -$: indicator of loading sense object : for reinforced concrete members

energy (see Table 4). Even though the various numerical factors in the damage index were obtained from the regression of numerous experimental data, the damage model was represented by a linear combination of damages caused by the maximum deformation and the hysteretic energy dissipation during earthquake. This linear summation resulted in a discrepancy, because these two variables were linearly independent.

One of the most frequently used approaches for overall damage assessment is performed by a combination of weighting factors of local damage indices (see Table 5). Bertero and Bresler⁽⁴⁾ suggested a global damage index based on the ductility ratio of elements, which is a weighted assemblage of the local damage indices. Park et al.⁽¹⁷⁾ also used the weighted combination of individual member's damage contents to establish the overall damage index, using

Table 4. Local damage indices based on linear combination of ductility ratio and dissipated energy

Proposer	Equation	Remarks
Park, Ang & Wen (1984)	$D_e = \frac{\delta_{max}}{\delta_u} + \frac{\beta}{Q_y \delta_u} \int dE$	D_e : damage index δ_{max} : maximum deformation experienced so far δ_u : ultimate deformation under monotonic loading Q_y : calculated yield strength dE : dissipated energy increment β : non-negative parameter object : for reinforced concrete members
Mizuhata Nishigaki (1987)	$D_k(n) = \frac{ \delta_{max} }{\delta_F} + \sum_{i=1}^k \frac{E_{ki}}{E_T}$	$D_k(n)$: damage index of member k : number of cycles δ_{max} : maximum displacement experienced δ_F : displacement at failure under monotonic loading E_{ki} : dissipated energy in the i -th cycle E_T : total dissipated energy object : for reinforced concrete members

Table 5. Global damage indices based on ductility ratio or dissipated energy

Related Variable	Proposer	Equation	Remarks
Ductility ratio	Bertero & Bresler (1977)	$D_i = \frac{1}{\sum w_i} \cdot \left(\sum_{i=1}^n \frac{w_i \gamma d_i}{\chi_i c_i} \right)$	D_i : cumulative damage index w_i : important weighting factor for i -th structural component χ_i : service history influence coefficient for demand γ_i : service history influence coefficient for capacity d_i : response(demand) of the element i c_i : resistance (capacity) of the element i object : for reinforced concrete structures
	Roufaiel & Meyer (1987)	$GDP = \frac{d_R - d_y}{d_F - d_y}$	GDP : global damage parameter d_R : maximum roof displacement d_y : roof displacement at the yield of the first member d_F : roof displacement at the failure structure object : for reinforced concrete structures
Dissipated energy	Park & Paulay (1975)	$D_{Sk} = \frac{\sum_{i=1}^{n_k} D_i^k \cdot E_i^k}{\sum_{i=1}^{n_k} E_i^k}$ $D_g = \sum_{k=1}^N D_{Sk} I_k$	D_{Sk} : damage index for k story D_i^k : damage index of joint i in the story k n_k : number of potential plastic hinges in k -th story E_i^k : energy dissipated in joint i of story k N : total number of stories $I_k = \frac{N+1-k}{N}$: weighting factor for story k object : for reinforced concrete structures
	Park, Ang & Wen (1985)	$D_g = \frac{\sum_i D_i^k E_i}{\sum_i E_i}$	D_g : global damage index E_i : total energy dissipated by the i -th member D_i^k : local damage index of i -th member object : for reinforced concrete structures

the energy absorbing capacity. The other approaches for global damage assessment were performed in applying ductility ratio and dissipated energy by Roufaiel and Meyer⁽⁹⁾ and Park and Paulay⁽¹⁸⁾, respectively.

Structural behavior and damage process under earthquake loading are very complex phenomena which are very difficult to model analytically or to reproduce in laboratory experiments. The literatures regarding the damage models are very vast, as indicated in Tables 1~5. The common approaches to seismic damage assessment are based on the concepts of Manson-Coffin hypothesis, ductility and stiffness ratios, or dissipated energy hypothesis for low-cycle fatigue. But the states of damage and failure in structures and their members are not yet definite. A clear definition for damage and failure of structural members under severe cyclic loading is required. Almost all of these past models have disregarded local instability phenomena in the plastic regions of member related to damage and failure caused by earthquake loads.

3. Failure Criteria for Steel Members under Strong Excitations

A fundamental condition of repeated loading is that the amplitude of the induced displacement or strain is constant. The amplitude a increases, the number of F of the loading cycles that can be applied up to the fatigue failure decreases. The Manson-Coffin rule stipulates a relationship

similar to what is known as the S-N curve or Wöhler curve, which represents graphically the relation of stress(S) and the number of cycles(N) at failure of the material. This rule relates $\log a$ and $\log F$ linearly with a negative factor, as shown in Fig. 1, and is expressed as

$$a = bF^j \quad (1)$$

where b and j are material constants. However, it seems meaningless to compare the abundant numerical expressions for the relationship of the Manson-Coffin rule obtained from each test, because the respective definitions of a failure state and the materials of the test specimens vary. It is proposed in formulating the failure criterion that the number F should be replaced by the total energy dissipated or by an effective number equal to the total energy divided by the energy absorbed per cycle in a stationary process. The evaluation of the deformation amplitude is based either on the difference between the maximum and minimum deformation or on its residual component, which taken to be the difference in the deformations corresponding to the vanishing load⁽¹⁹⁾.

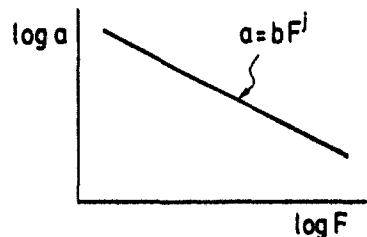


Fig. 1 The Manson-Coffin rule

In order to represent quantitatively structural damage and failure for structural members subjected to earthquake loads, a clear definition of failure for structures and their components under repeated loading is required. Because failure mechanisms are often associated with very complex physical phenomena, however, it is difficult to describe the failure state definitely. There are basically five different approaches to define failure state for members subjected to cyclic loading : (1) the initiation of surface cracking⁽²⁰⁾, (2) the crack tip opening displacement(CTOD) criterion⁽²¹⁾, (3) the occurrence of severe cracking⁽²²⁾, (4) the strength drop reaching below a certain value of the initial yield stress⁽²³⁾, and (5) the complete rupture of the cross-section. But the state of failure for structural steel members under strong seismic excitations is not as yet definitive.

4. Experimental and Numerical Observations on Seismic Failure Behavior of Steel Members

Past studies using experiments on steel structural members, including columns, beams, and braces, commonly report that global buckling of steel members can easily trigger local buckling of thin-plate elements. The local buckling causes concentrated large plastic deformations, which within 5 to 20 loading cycles induce cracking that eventually leads to rupture of members. Also, it has been observed

that seismic loading of steel members has caused ruptures at local buckling locations. Some of previous researchers have classified this type of failure as low-cycle fatigue. However, fatigue generally means a failure caused by crack propagation without macroscopic deformations⁽²²⁾. Therefore, classifying failures that occur under repeated large deformations, such as those in this study, as belonging the category of fatigue failure is questionable. It is proposed that this phenomenon should be called very low cycle failure⁽¹⁾.

To clarify the damage process leading to cracking under very low cycle loading, it is required to discuss global member performance and local material behavior. The writers performed some tests (see Fig. 2) to observe cracking behavior of

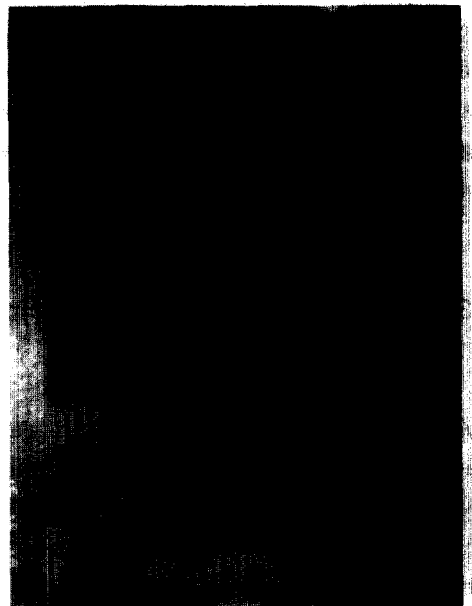


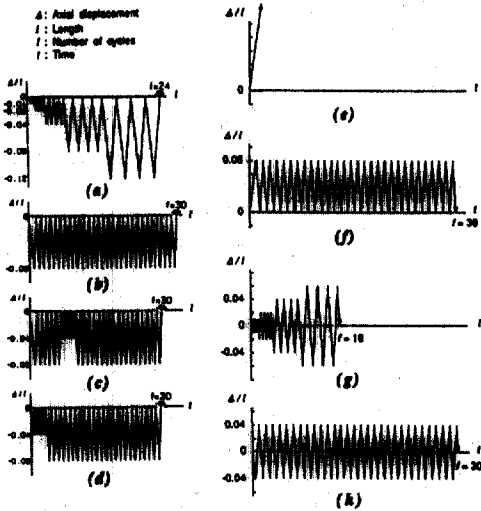
Fig. 2 Local deformation and cracking of the steel angle member

steel members that experienced localized and large deformation caused by buckling⁽¹⁾. The experiments were performed with special attention to the inelastic post-buckling behavior of steel angles and the state of cumulative plastic strains at the critical part of the specimen. Two types of angles L-40×40×3 and L-40×40×5, SS400 grade steel, served as specimens. The yield stress and the ultimate tensile strength of the materials were 331-371 N/mm² and 447-469N/mm², respectively. A total of 28 specimens was tested. Each specimen was pin-supported, as shown in

Fig. 2. The effective length ℓ , the tested part between the pin-supports, was 318 mm(or 300mm) or 618mm, as indicated in Table 6. Test parameters are summarized as follows: (1) slenderness ratio λ ; (2) width-to-thickness ratio b/t ; (3) loading pattern; and (4) deflection mode. The λ -value of the specimens ranged between 37 and 41 or equalled 77. The ratio b/t was 8.6 or within the range of 13.3-16.4, as shown in Table 6. To investigate the quantitative effect of the important factors on the very low cycle failure process, a wide range of loading histories

Table 6. Specimen sizes and test parameters

Specimen name (1)	Length ℓ (mm) (2)	Width b (mm) (3)	Thickness t (mm) (4)	Slenderness ratio λ (5)	Width-to-thickness ratio b/t (6)	Loading pattern (7)	Deflection mode (8)
L3IP	318	39.6	2.80	40.5	14.1	LI	P
L3IN	301	40.4	2.55	37.4	15.8	LI	N
L3CP _a	300	40.3	2.55	37.3	15.8	LC	P
L3CP _b	318	39.6	2.83	40.5	14.0	LC	P
L3CN	301	40.5	2.47	37.4	16.4	LC	N
L3GP	318	39.5	2.80	40.5	14.1	LG	P
L3SP	318	39.5	2.82	40.5	14.0	LS	P
L3GN	318	39.5	2.78	40.5	14.2	LG	N
L3SN	318	39.6	2.79	40.5	14.2	LS	N
L5IP	318	39.2	4.56	41.4	8.6	LI	P
L5IN	300	39.2	4.58	39.0	8.6	LI	N
L5CP _c	317	39.3	4.55	41.2	8.6	LC	P
L5CP _b	317	39.2	4.55	41.2	8.6	LC	P
L5CN	318	39.2	4.55	41.4	8.6	LC	N
H3IP	618	40.3	2.49	76.8	16.2	LI	P
H3IN	618	40.2	2.50	76.8	16.1	LI	N
H3CP	618	40.3	2.50	76.8	16.1	LC	P
H3CN	618	40.4	2.50	76.8	16.2	LC	N
H3GP	618	40.2	2.51	76.8	16.0	LG	P
H3SP	618	40.4	2.49	76.8	16.2	LS	P
T3M	316	39.7	2.97	40.4	13.4	TM	-
T3CP _a	315	39.6	2.98	40.3	13.3	TC	P
T3CP _b	316	39.7	2.97	40.4	13.4	TC	P
T3CN	318	39.6	2.97	40.7	13.3	TC	N
A3CP	316	39.7	2.99	40.4	13.3	AC	P
A3CN	315	39.6	2.97	40.3	13.3	AC	N
A3IP	316	39.7	2.98	40.4	13.3	AI	P
A3IN	315	39.5	2.96	40.3	13.3	AI	N



- (a) LI-type(contraction side)
- (b) LC-type(contraction side)
- (c) LG-type(contraction side)
- (d) LS-type(contraction side)
- (e) TM-type(elongation side)
- (f) TC-type(elongation side)
- (g) AI-type(alternate)
- (h) AC-type (alternate)

Fig. 3 Loading patterns

was adopted, as shown in Fig. 3. Namely, the choices in Fig. 3 included increasing displacement amplitude (LI and AI types), constant displacement amplitude (LC, TC, and AC types), stepwise varying displacement amplitude (LG and LS types), and monotonic elongation (TM type), in the relative axial displacement Δ . The total number of load cycles was set in the loading program up to 16, 24, or 30. The experiments were performed up to the occurrence of visible cracks or rupture of the specimen. When a steel angle buckled due to the initial compressive loading, two types of buckling deflection modes were observed. Therefore, the deflection mode

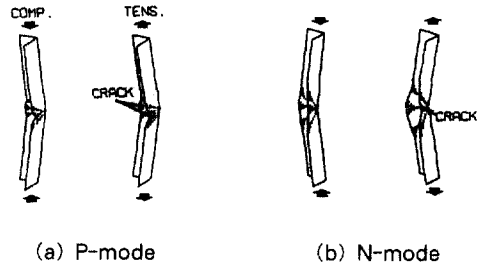


Fig. 4 Deflection Modes

played an important role as a testing parameter. Positive deflection mode (P-mode) and negative deflection mode (N-mode) are defined as shown in Fig. 4 (a and b), respectively.

A slowly varying uniaxial load was applied to the specimen using a hydraulic servo-actuator with a loading capacity of 294 kN. A very small eccentricity, about $\pm 0.5\text{mm}$, was given in the load to control the deflection mode. Loading was controlled by the relative axial displacement Δ between the pin-supports, programmed in the contraction side (L and H series), the elongation side (T series), or in the both sides (A series), as shown in Table 6. This causes buckling in the specimen under the initial compressive loading.

Steel angles are composed of two simply thin-plates. The angles experience the fundamental failure modes, i.e. failure caused by pure tension, compression and bending, and tension and bending, due to elongation and global bending and local buckling deformations under very-low-cycle loading. Also, by using the steel angles, it is expected that structural factor like the width-to-thickness ratio might be clearly defined and the

structural fatigue behavior after global flexural buckling and local buckling might be investigated under the severe cyclic loading. This is motivation which chosen the steel angle specimens from standard structural shapes. Namely, even though the test specimens in this study are the steel angles, the aim of experiment is to investigate comprehensively the plastic failure behavior of thin-walled steel members under repeated loading rather than that of angles solely. Thus this experiment will provide an useful data to clarify the complicated failure behavior for structural members which are subjected to the fundamental phase such as the pure elongation and the compressive-bending and tensile-bending deformations due to repeated loads.

During testing, positive or negative deflection was observed as defined in Fig. 4. In the case of P-mode deflection, the global buckling deformation was accompanied by large deformation due to local buckling of the leg plates at the midheight of the specimen as shown in Fig. 5. In the case of N-mode deflection, only the global

buckling was observed. These buckling deformations induces very large local strains at the critical midpart. The test results, for steel angle members under very low cycle loading, have shown that inelastic buckling caused a sudden decrease in the compressive load-carrying capacity, but only a slight decrease in the succeeding tensile load-carrying capacity (see Fig. 5). However, both the compressive and tensile load-carrying capacities were considerably decreased by the initiation of cracking. It is thus found that ultimate state of failure is closely related to the occurrence of a visible crack. In this investigation, therefore, the failure state for steel members under earthquake loading is characterized by the initiation of surface cracking. Fig. 6 shows typical axial stress-

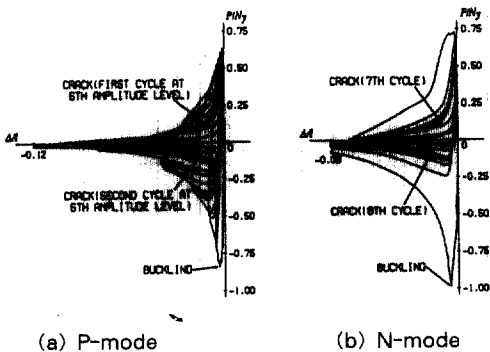
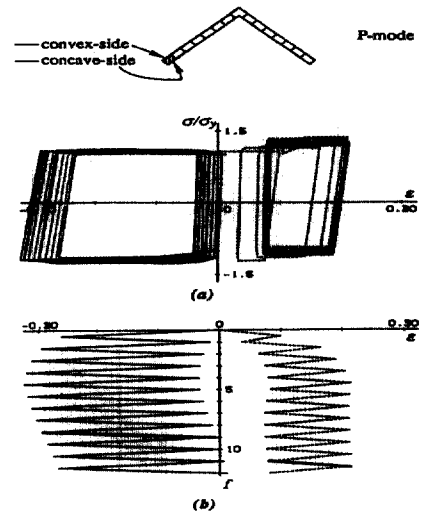


Fig. 5 Typical load-axial displacement relations



(a) Local stress-strain hysteresis
(b) Local strain history with increasing number of cycles

Fig. 6 Typical steel angle model

strain hysteresis and the corresponding strain history with increasing number of cycles. This hysteresis curve and historical data give information for the extreme fibers of the concave and convex sides of the bending deformation at the mid-cross-section elements (see Fig. 1). This indicates that the critical element of the angle model under the very low cycle loading has undergone very large plastic strain reversal. As shown in Fig. 6, the amplitude of local strain variation in the absolute value was approximately 25~35% in each cycle on the concave-side surface and 15~20% on the convex surface. Thus the strain amplitude on the concave-side surface was larger than that on the convex-side surface. This may be attributed to locally severe straining as shown in Fig. 4. This means that the most severe cycling of local strain occurs at the concave-side surface of the global and/or local buckling deformation. It can be considered this corresponds to the experimental phenomenon that the first

cracking was always observed on the concave-side surface of the buckling deformation (see Fig. 6).

The thick bold lines in Fig. 6(b) indicate the cracking cycles in which cracks were observed in the corresponding test specimens. The total cumulative plastic components of local strain in the tensile stress side in each cycle were calculated up to the cracking cycle. This resulted in the values of 104~255% for the simulated cases, which have the same order of magnitude as in the monotonic-tensile tests⁽¹⁾. Therefore, the local strain information might be used to represent cracking due to the cumulative damage under severe seismic loading.

5. Seismic Damage Model for Structural Steel Members

The approaches to seismic damage estimation are often based upon the energy dissipation capacity. But the energy dissipation process and capacity depend

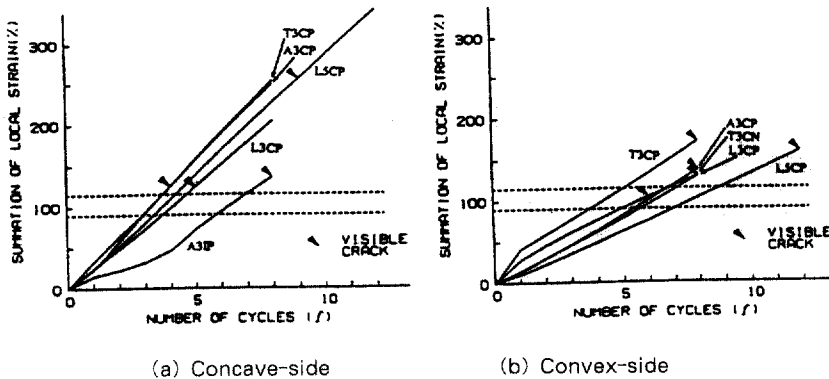


Fig. 7 Cumulative plastic local strain with increasing number of cycles

heavily on the loading history and failure mode. Therefore, it may be impossible that the damaged state under inelastic cyclic loading is clearly represented by a simple one-to-one correspondence between dissipated energy capacity and physical damage such as the outbreak of crack. Fig. 7 presents the relations between the summation of cumulative local strain in the critical cross-section and the increasing number of cycles for all the models obtained from the analysis. Here the lower and upper dash lines correspond to 90% and 115% of the residual local strain at the ruptured portion under monotonic-tensile testing, respectively. Based upon the failure definition described in the above section and the result of Fig. 7, a new damage model for structural steel members under severe cyclic loading can be suggested. The new method may be described by the cumulative value of the critical local strain in the course of increasing number of cycles, which is conservatively compared with the threshold value 90% of the local strain at the ruptured portion under the pure monotonic-tensile angle and material testing. That is, the failure state is indicated if the cumulative value of the local strain in the critical cross-section exceeds the limit strain of 90%. Thus, the damage indicator under cyclic excitations as in strong earthquakes may be formulated as follows:

$$\text{If } \sum_{i=1}^N \epsilon_i \geq \epsilon_{limit}, \text{ then failure state (2)}$$

and

$$\text{If } \sum_{i=1}^N \epsilon_i < \epsilon_{limit}, \text{ then no failure state (3)}$$

where N , ϵ and ϵ_{limit} are the number of cycles, the local strain in the critical cross-section and the limit strain, respectively. The value of ϵ_{limit} might be 90% in the case of structural steel members under the severe seismic loading.

In general, the local strain history may be calculated by the numerical approach using finite element analysis with material nonlinear and geometric nonlinear effects. From Eqs. (2) and (3), the damage model "D" of steel member to "N" cycles can be determined by the normalized form as follows:

$$D = \sum_{i=1}^N \left(\frac{\epsilon_i}{\epsilon_{limit}} \right) \quad (4)$$

Therefore, $D \geq 1$ indicates the failure state, while $D < 1$ denotes a degree of damage at the corresponding loading step. As indicated in Fig. 5, the increment in damage indicators as function of the number of increasing cycles can be observed. The failure state, i.e. the initiation of cracking, for all the models may be detected at the calculated damage indicator in the order of 1.2~1.5. It might be, therefore, considered that the threshold local strain 90% corresponds to the occurrence of the ultimate failure for steel members due to cyclic loads such as strong seismic loads.

6. Conclusions

From this survey of the literatures, it was apparent that the common approaches to seismic damage models were based on the concepts of Manson-Coffin hypothesis, ductility and stiffness ratios, or dissipated energy hypothesis. There was five approaches to define the failure state, i.e. the initiation of surface cracking, the crack tip opening displacement criterion, the occurrence of severe cracking, the strength drop reaching below a certain value of the initial yield stress, and the complete rupture of the cross-section. A failure criterion related to the initiation of surface cracking was described, which applied for the failure definition for steel members under inelastic cyclic loading as in strong earthquakes. Based on a series of the experimental and numerical investigations using steel angle members subjected to the very low cycle loading, a new approach to seismic damage assessment for steel members has been proposed in conjunction with the suggested definition of failure. This new damage model might be described by the cumulative value of the critical local strain in the course of increasing number of cycles, which is compared with the threshold value 90% of the residual local strain at the ruptured portion under the monotonic-tensile material testing. With respect to further research, the experimental and analytical investigations for structural steel members having various shapes under very low cycle loading may be needed to verify the

proposed seismic damage model.

Acknowledgement

This research investigation is supported by 1997 Research Funds of Pohang Iron & Steel Company under Grant 97K029. The writers are grateful for this support.

References

- (1) Y.-S. Park : Damage Process of Steel Members under Very-Low-Cycle Loading, Thesis of Doctor of Engineering, Kyoto University, Japan, 1993.
- (2) J. T. P. Yao and W. H. Munse : Low-Cycle Fatigue Behavior of Mild Steel, Special Technical Publication No. 338, American Society for Testing and Materials, Pa., 1962, pp. 5-24.
- (3) I. Kasiraj and J. T. P. Yao : Fatigue Damage in Seismic Structures, Jour. of Structural Division, ASCE, Vol. 95, No. ST8, 1969, pp. 1673-1692.
- (4) V. V. Bertero and B. Bresler : Design and Engineering Decisions-Failure Criteria (Limit States), Report No. UCB/EERC-77/06, University of California, Berkeley, California, 1977, pp. 117-142.
- (5) T. Blejwas and B. Bresler : Damage-ability in Existing Building, Report No. UCB/EERC-78/12, University of California, Berkeley, California, 1979.
- (6) J. E. Stephens and J. T. P. Yao : Damage Assessment using Response Measurements, Jour. of Structural Engineering, ASCE, Vol. 113, No. 4, 1987, pp. 787-801.
- (7) J. M. Lybas and M. A. Sozen : Effect of Beam Strength and Stiffness on Dynamic Behavior of Reinforced Concrete Coupled Walls, Structural Research Series No. 444, Department of Civil Engineering,

University of Illinois, Urbana-Champaign, 1977.

- (8) C. Meyer and M. S. L. Roufaiel : Reliability of Damaged Reinforced Concrete Frames, Proc. of 8th World Conference on Earthquake Engineering, San Francisco, California, U.S.A., Vol. 4, 1984, pp. 535-542.
- (9) M. S. L. Roufaiel and C. Meyer : Reliability of Concrete Frames Damaged by Earthquakes, Jour. of Structural Engineering, ASCE, Vol. 113, No. 3, 1987, pp. 445-457.
- (10) N. K. Gosain, R. H. Brown and J. O. Jirsa : Shear Requirements for Load Reversals on RC Members, Jour. of Structural Division, ASCE, Vol. 103, No. ST7, 1977, pp. 1461-1476.
- (11) H. Banon, J. M. Biggs and H. M. Irvine : Seismic Damage in Reinforced Concrete Frames, Jour. of Structural Division, ASCE, Vol. 107, No. ST9, 1981, pp. 1713-1729.
- (12) T. H. Hwang and C. F. Scribner : R/C Member Cyclic Response during Various Loadings, Jour. of Structural Engineering, ASCE, Vol. 110, No. 3, 1984, pp. 477-489.
- (13) D. Darwin and C. K. Nmai : Energy Dissipation in RC Beams under Cyclic Load, Jour. of Structural Engineering, ASCE, Vol. 112, No. 8, 1986, pp. 1829-1846.
- (14) Y. S. Chung, M. Shinozuka and C. Meyer : Automated Seismic Design of Reinforced Concrete Building, Technical Report NCEER-88-0024, National Center for Earthquake Engineering Research, New York, 1988.
- (15) Y.-J. Park, A. H.-S. Ang and Y. K. Wen : Seismic Damage Analysis and Damage-limiting Design of R.C. Buildings, Structural Research Series No. 516, Department of Civil Engineering, University of Illinois, Urbana-Champaign, 1984.
- (16) T. Nishigaki and K. Mizuhata : Evaluation of Seismic Safety for Reinforced Concrete Structures, Trans. of Architectural Institute of Japan, No. 332, 1983, pp. 19-29(in Japanese).
- (17) Y.-J. Park, A. H.-S. Ang and Y. K. Wen : Damage-Limiting Design of Buildings, Earthquake Spectra, Vol. 3, No. 1, 1987, pp. 1-26.
- (18) R. Park and T. Paulay : Reinforced Concrete Structures, John Wiley & Sons, New York, 1975.
- (19) T. Nonaka and S. Iwai : Failure of Bar Structures under Repeated Loading, Structural Failure(edited by T. Weirzbicki and N. Jones), John Wiley & Sons, 1988, pp. 389-433.
- (20) H. Goto, H. Kameda, Y. Koike, R. Izunami, K. Wakita and Y. Sugihara : A Consideration on Failure Process of Structural Steel under Repeated Flexural Loads, Annuals of Disaster Prevention Research Institute, Kyoto University, No. 17B, 1974, pp. 157-169(in Japanese).
- (21) R. M. Caddell : Deformation and Fracture of Solids, Prentice-Hall Inc., 1980.
- (22) S. T. Rolfe and J. M. Barsom : Fracture and Fatigue Control in Structures (Application of Fracture Mechanics), Prentice-Hall Inc., 1977.
- (23) M. B. Atalay and J. Penzien : The Seismic Behavior of Critical Regions of Reinforced Concrete Components as Influenced by Moment, Shear and Axial Forces, Report No. EERC 75-19, University of California, Berkeley, California, 1975.

(접수일자 : 1998년 5월 25일)